This article has been accepted for publication in a future issue of this journal, but has not been fully edited. Content may change prior to final publication. Citation information: DOI 10.1109/TMECH.2021.3087193, IEEE/ASME Transactions on Mechatronics

Aggressive maneuver oriented robust actuator fault estimation of a 3-DOF helicopter prototype considering measurement noises

Tianzhen Wang, *Senior member*, *IEEE*, Mengjie Lu,
Xiaoyuan Zhu, *member*, *IEEE*, Ron J. Patton, *Life Fellow*, *IEEE*

***Abstract*—This paper presents a robust actuator fault estimation strategy design for a 3-DOF helicopter prototype which can be adapted to aggressive maneuvers. First, considering large pitch angle condition during flight, nonlinear coupling characteristic of the helicopter system is exploited. As the pitch angle can be measured in real time, a polytopic linear parameter-varying (LPV) model is developed for the helicopter system. Furthermore, considering measurement noises in the actual helicopter system, the dynamical model of helicopter system is modified accordingly. Then, based on the modified polytopic LPV model, a robust unknown input observer (UIO) is developed for the helicopter system to realize actuator fault estimation, in which both measurement noises and large pitch angle are considered. Robust performance of proposed fault estimation approach is guaranteed by using energy-to-energy strategy. And the observer gains are calculated by using linear matrix inequalities. Finally, based on a 3-DOF helicopter prototype, both simulations and experiments are conducted. The effects of measurement noises and large pitch angle on the fault estimation performance are sufficiently demonstrated. And effectiveness as well as advantages of the proposed observer is verified by using comparative analysis.**

***Index Terms*—fault estimation, measurement noises, aggressive maneuvers, 3-DOF helicopter, comparative experiments.**

I. Introduction

As one kind of typical rotor unmanned aerial vehicle (UAV), unmanned helicopter is widely used in many field, which can provide wireless coverage, search and rescue, delivery of goods, security and surveillance[1][2][3]. Because the helicopter is a highly complex system, system failures are generally hard to be averted. In addition, as the helicopter is an nonlinear and unstable system, any actuator or sensor fault will result in disastrous consequences[4][5]. Therefore, in order to get the fault information at an early stage, it is of great importance to conduct fault estimation (FE) for helicopter system[6][7][8].

This work was supported the National Natural Science Foundation of China under Grant 51605278 and 61673260 (corresponding author: Xiaoyuan Zhu)

Tianzhen Wang and Mengjie Lu are with the School of Logistics Engineering, Shanghai Maritime University, Shanghai 201306, China

Xiaoyuan Zhu is with the School of Mechanical Engineering, Southeast University, Nanjing 211189, China (e-mail: zhuxyc@gmail.com).

Ron J. Patton is with the School of Engineering and Computer Science, University of Hull, Hull HU6 7RX, U.K.

Nowadays, many fault estimation approaches have been presented, such as proportional integral observer (PIO)[9], adaptive observer [10], unknown input observer (UIO)[11][12], learning observer[13], sliding mode observer (SMO)[14], Kalman filter (KF)[15], and etc. For the fault estimation design of helicopter system, an adaptive fault estimation approach for a quadrotor in [16], by using which invariant faults can be estimated. Zhong et al.[17] presented an interacting multiple model algorithm for unmanned quadrotor helicopter to detect, isolate and estimate multiple actuator and sensor faults simultaneously. Abbaspour et al.[18] developed a neural adaptive observer to achieve sensor and actuator fault estimation of UAV systems, which can estimate abrupt, intermittent, and incipient faults accurately. Nian et al.[19] proposed a robust adaptive fault estimation approach for a quadrotor considering external disturbances. Chen et al. [20] develop an adaptive SMO for actuator fault estimation of a non-linear helicopter system. A radial basis function neural network based disturbance observer is proposed in [21] to realize actuator faults estimation, in which system uncertainties are taken into consideration. Similarly, a high order sliding mode observation is developed in [22] for a 3-DOF helicopter prototype to realize actuator fault estimation. An adaptive nonlinear observer is designed in [23] to simultaneously realize actuator and sensor faults estimation of 3-DOF laboratory helicopter, which can accurately estimate abrupt faults under square and sinusoidal references trajectory tracking. A non-linear UIO is presented in [24] to simultaneously realize state and actuator fault estimation. These fault estimation approaches are proven to be effective and show good performance for helicopter system. However, they are all limited to numerical simulations, in which experimental verifications are expected to be further exploited. However, as actual helicopter platform is costly and fragile, and more prone to accidents in the event of failure, sufficient validations for various fault estimation methods are generally difficult to conduct[25][26]. Thus, to solve this problem, some specially designed test benches have been developed, such as Quanser's helicopter platform. These test platforms are easy to operate and have the basic dynamic characteristics of an actual helicopter system. A comparative fault estimation study of 3-DOF helicopter is presented in [27], in which both simulation and experimental tests are given. However, the measurement

1083-4435 (c) 2021 IEEE. Personal use is permitted, but republication/redistribution requires IEEE permission. See http://www.ieee.org/publications_standards/publications/rights/index.html for more information.

This article has been accepted for publication in a future issue of this journal, but has not been fully edited. Content may change prior to final publication. Citation information: DOI 10.1109/TMECH.2021.3087193, IEEE/ASME Transactions on Mechatronics

noise is not considered.

In practical engineering applications, measurement noises are generally inevitable, which has a great impact on the performance of model-based fault estimation methods. However, measurement noises are generally not considered in many fault estimation approaches[12][13][14]. Thus, it can be concluded that performance and even effectiveness of these fault estimation approaches will be largely affected when applied to practical systems. In order to deal with the measurement noises, some theoretical research works were also proposed. Gao et al.[30] presented a modified PID observer to realize simultaneous states, input disturbance, and measurement noise estimation. Based on which, a high-gain observer is developed in [31] to further realize actuator and sensor faults estimation simultaneously. Considering output noise, a modified L_1 adaptive descriptor observer is presented in [32] to realize simultaneous system state and output noise estimation. These fault estimation approaches are expected to be further validated by using experimental tests, which also provide good reference to the fault estimation design of 3-DOF helicopter system considering measurement noises.

Helicopter system is characterized with high maneuverability, which often operates in aggressive missions and harsh environments[33][34]. However, most of existing researches on fault estimation of 3-DOF helicopter always assume that the helicopter system works in mild maneuvers, that is, the pitch angle is very small[22][24][35]. The 3-DOF helicopter platform has many of the characteristics of real helicopters, which can also easily realize aggressive maneuvers by using large pitch angle. As there is nonlinear coupling between the elevation and pitch axis, the nonlinear coupling effects will largely increase with large pitch angle. Thus, it will be more challenging to conduct fault estimation of the 3-DOF helicopter porotype under large pitch angle. As the pitch angle can be measured in the 3-DOF helicopter platform, linear parameter varying (LPV) modeling approach is adopted to handle the interaxis nonlinear coupling problem in aggressive maneuvers[36][37]. And the main contributions of this paper can be summarized as follows

(1) Aggressive maneuvers are considered in the robust fault observer design for the helicopter system. A polytopic LPV model for 3-DOF helicopter is established to deal with the interaxis nonlinear coupling, which caused by the large pitch angle during the flight.

(2) Measurement noises are considered in fault estimation design of the 3-DOF helicopter. Based on the polytopic LPV model of the helicopter system, a robust UIO is developed to realize actuator fault estimation, in which both measurement noises and large pitch angle are considered.

(3) Based on a 3-DOF helicopter prototype, comparative analysis with high gain observer and modified PID observer are conducted. And the effectiveness as performance of proposed fault observer design is validated by using both simulations and experiments.

The rest of the paper is structured as follows. A polytopic LPV model is built for the 3-DOF helicopter prototype in Section II. Robust fault estimation is developed in Section III. Simulation and experimental results illustrating the performance of proposed observer design are demonstrated in Section IV, and conclusions are given in Section V.

II. Problem Formulation

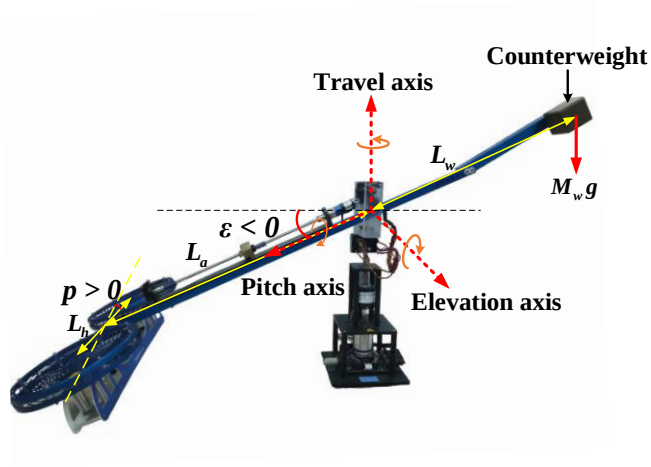

Fig 1. 3-DOF helicopter porotype from Quanser Company.

The 3-DOF helicopter porotype from Quanser Company is presented in Fig 1. Two DC motors are adopted to drive the front and back propellers respectively, which control the three dimensional rotational motions, i.e. the evaluation, pitch and travel motion of the helicopter. The body frame and the counterweight are jointed via the arm, and are supported by the base. The counterweight is used to decrease the motor thrust needed to lift the helicopter.

The dynamic model of the helicopter system is developed as follows[28][29].

$$\begin{aligned} J_\varepsilon \ddot{\varepsilon} &= K_f L_a \cos p\left(V_f + V_b\right) - (M_h L_a - M_w L_w) g \cos\varepsilon + w_\varepsilon \\ J_p \ddot{p} &= K_f L_h \left(V_f - V_b\right) + w_p \\ J_t \ddot{t} &= K_f L_a \sin p \cos\varepsilon \left(V_f + V_b\right) + K_f L_h \sin\varepsilon \left(V_f - V_b\right) + w_t \end{aligned} \tag{1}$$

where J_i and w_i are inertia moments and external disturbances, where the subscript $i = \varepsilon, p, t$ represent the elevation, pitch, and travel respectively. V_f and V_b are the respective voltages applied to the front and back motors, K_f is propeller force-thrust coefficient, M_h is the mass of the helicopter, including the fuselage, two propeller components and encoder, M_w is the mass of the counterweight, L_a is the distance from elevation axis to helicopter body, L_w is the distance from elevation axis to counterweight, L_h is the distance from each motor to pitch axis.

Considering the elevation and pitch motion only, dynamical model of the helicopter can be rewritten as

1083-4435 (c) 2021 IEEE. Personal use is permitted, but republication/redistribution requires IEEE permission. See http://www.ieee.org/publications_standards/publications/rights/index.html for more information.

This article has been accepted for publication in a future issue of this journal, but has not been fully edited. Content may change prior to final publication. Citation information: DOI 10.1109/TMECH.2021.3087193, IEEE/ASME Transactions on Mechatronics

$$\begin{aligned}
&\ddot{\varepsilon} = b_\varepsilon \cos(p)\left(V_f + V_b\right) + g_1(x) + d_\varepsilon \\
&\ddot{p} = b_p\left(V_f - V_b\right) + d_p \\
&b_\varepsilon = K_f L_a / J_\varepsilon, d_\varepsilon = w_\varepsilon / J_\varepsilon \\
&b_p = K_f L_h / J_p, d_p = w_p / J_p \\
&g_1(x) = -\frac{(M_h L_a - M_w L_w)g}{J_\varepsilon}\cos(\varepsilon)
\end{aligned} \tag{2}$$

where d_i is the system uncertainties, where the subscript $i = \varepsilon, p$ represent elevation and pitch respectively.

Define the system state vector as $x = \begin{bmatrix} x_1 & x_2 & x_3 & x_4 \end{bmatrix}^T = \begin{bmatrix} \varepsilon & p & \dot{\varepsilon} & \dot{p} \end{bmatrix}^T$, the output vector as $y = \begin{bmatrix} \varepsilon & p & \dot{\varepsilon} & \dot{p} \end{bmatrix}^T$, and the input vector as $u = \begin{bmatrix} V_f & V_b \end{bmatrix}^T$. The fault vector is $f_a = \begin{bmatrix} f_{a1} & f_{a2} \end{bmatrix}^T$, where f_{a1} and f_{a2} respectively represent the unknown faults of the front and back motors.

Assumption 1: The faults f_{a1}, f_{a2} and their first-order derivatives are bounded and belong to $L_2[0,\infty]$.

Considering actuator faults and measurement noises, dynamical model of the helicopter system can be further written as

$$\begin{aligned}
&\dot{x}(t) = Ax(t) + B(u(t) + f_a(t)) + g(x,t) + Dd(t) \\
&y(t) = Cx(t) + \omega(t)
\end{aligned} \tag{3}$$

where $\omega(t) \in R^4$ is the system measurement noise vector, $d(t) = \begin{bmatrix} d_\varepsilon & d_p \end{bmatrix}^T$ and

$$A = \begin{bmatrix} 0 & 0 & 1 & 0 \\ 0 & 0 & 0 & 1 \\ 0 & 0 & 0 & 0 \\ 0 & 0 & 0 & 0 \end{bmatrix}, B = \begin{bmatrix} 0 & 0 \\ 0 & 0 \\ b_\varepsilon \cos p & b_\varepsilon \cos p \\ b_p & -b_p \end{bmatrix},$$

$$C = \begin{bmatrix} 1 & 0 & 0 & 0 \\ 0 & 1 & 0 & 0 \\ 0 & 0 & 1 & 0 \\ 0 & 0 & 0 & 1 \end{bmatrix}, D = \begin{bmatrix} 0 & 0 \\ 0 & 0 \\ 1 & 0 \\ 0 & 1 \end{bmatrix}, g(x,t) = \begin{bmatrix} 0 \\ 0 \\ g_1(x,t) \\ 0 \end{bmatrix}.$$

Assumption 2: The nonlinear term $g(x,t)$ holds the following Lipschitz condition[24]

$$\left\| g(x_1,t) - g(x_2,t) \right\| \le \theta \left\| x_1 - x_2 \right\|, \forall x_1, x_2 \in R^4$$

where θ is the Lipschitz constant.

Remark 1: It can be seen from (3) that the nonlinear term $g(x,t)$ satisfies the condition of Assumption 2, and the Lipschitz constant is $\theta = (M_h L_a - M_w L_w)g / J_\varepsilon$.

As the pitch angle of 3-DOF helicopter platform is mechanically constrained within $[-\pi/4, \pi/4]$, following constraints are used in this paper as

$$p_{\min} \le p \le p_{\max}, p_{\min} = 0, p_{\max} = \pi/4 \tag{4}$$

The scheduling variable is chosen as $\alpha(t) = \cos(p)$

$$\alpha_{\min} \le \alpha \le \alpha_{\max}, \alpha_{\min} = 0.707, \alpha_{\max} = 1 \tag{5}$$

Since $p = p_{\min}$ for $\alpha = \alpha_{\max}$ and $p = p_{\max}$ for $\alpha = \alpha_{\min}$, the new parameter α can be used to describe the variation of p within its range.

Then, the LPV model of the 3-DOF helicopter system can be represented by

$$\begin{aligned}
&\dot{x}(t) = Ax(t) + B(\alpha)(u(t) + f_a(t)) + g(x,t) + Dd(t) \\
&y(t) = Cx(t) + \omega(t)
\end{aligned} \tag{6}$$

The matrix $B(\alpha)$ can be written as polytopic matrices and given by[38]

$$B(\alpha) = \sum_{i=1}^{2} \rho_i(\alpha) B_i \tag{7}$$

where $\rho_i(\alpha)$ are the weights of the LPV subsystems, it holds

$$\sum_{i=1}^{2} \rho_i(\alpha) = 1, 0 \le \rho_i(\alpha) \le 1$$

The polytopic representation of the system (6) becomes

$$\begin{aligned}
&\dot{x}(t) = \sum_{i=1}^{2} \rho_i(\alpha)(Ax(t) + B_i(u(t) + f_a(t)) + g(x,t) + Dd(t)) \\
&y(t) = Cx(t) + \omega(t)
\end{aligned} \tag{8}$$

where B_i is the time invariant matrix, the scalar membership functions are given by

$$\rho_1(\alpha) = \frac{1-\alpha}{0.293}, \rho_2(\alpha) = 1 - \rho_1(\alpha) \tag{9}$$

Remark 2: Different from the work in [27] and [35], a polytopic LPV model is developed for the 3-DOF helicopter system instead of linear model, which can better present the dynamical characteristics of the helicopter system.

III. Robust Fault Estimation Design

Based on the polytopic LPV fault model of 3-DOF helicopter, the UIO approach is adopted to estimate actuator fault.

A. System Augmentation

Define the augmented state as:

$$\bar{x} = \begin{bmatrix} x^T & f_a^T \end{bmatrix}^T \tag{10}$$

And the related augmented system model can be developed as follows:

$$\begin{aligned}
&\dot{\bar{x}}(t) = \sum_{i=1}^{2} \rho_i(\bar{A}_i \bar{x}(t) + \bar{B}_i u(t) + \bar{g}(A_0 \bar{x}, t) + \bar{D}\bar{d}(t)) \\
&y(t) = \bar{C}\bar{x}(t) + \omega(t)
\end{aligned} \tag{11}$$

where $\bar{d} = \begin{bmatrix} d & \dot{f}_a \end{bmatrix}^T$, and

$$\bar{A}_i = \begin{bmatrix} A & B_i \\ 0 & 0 \end{bmatrix}, \bar{B}_i = \begin{bmatrix} B_i \\ 0 \end{bmatrix}, \bar{D} = \begin{bmatrix} D & 0 \\ 0 & I_2 \end{bmatrix}, \bar{g}(A_0\bar{x}, t) = \begin{bmatrix} g(x,t) \\ 0 \end{bmatrix},$$

$$\bar{C} = \begin{bmatrix} C & 0 \end{bmatrix}, A_0 = \begin{bmatrix} I_4 & 0 \end{bmatrix}.$$

Remark 3: Different from the work in [27], measurement noise is considered in the fault estimation design of the 3-DOF helicopter system.

B. LPV Model based UIO Design

Considering the augmented system (11), the LPV model based UIO can be developed as following

1083-4435 (c) 2021 IEEE. Personal use is permitted, but republication/redistribution requires IEEE permission. See http://www.ieee.org/publications_standards/publications/rights/index.html for more information.

This article has been accepted for publication in a future issue of this journal, but has not been fully edited. Content may change prior to final publication. Citation information: DOI 10.1109/TMECH.2021.3087193, IEEE/ASME Transactions on Mechatronics

$$\begin{aligned}\dot{z}(t) &= \sum_{i=1}^{2}\rho_i(M_i z(t)+G_i u(t)+N_i\bar{g}(A_0\hat{\bar{x}},t)+L_i y(t))\\ \hat{\bar{x}}(t) &= z(t)+Hy(t)\end{aligned} \tag{12}$$

where $z\in R^6$ is the system state of the dynamics (12) and $\hat{\bar{x}}\in R^6$ is the estimation of $\bar{x}\in R^6$, observer gain matrices M_i, G_i, N_i, L_i, H are to be designed.

And the estimation error can be represented as

$$\begin{aligned}e(t) &= \bar{x}(t)-\hat{\bar{x}}(t)\\ &= \bar{x}(t)-z(t)-H\bar{C}\bar{x}(t)-H\omega(t)\\ &= (I_6-H\bar{C})\bar{x}(t)-z(t)-H\omega(t)\end{aligned} \tag{13}$$

According to (11)-(13), the derivative of $e(t)$ is

$$\begin{aligned}\dot{e}(t) &= (I_6-H\bar{C})\dot{\bar{x}}(t)-\dot{z}(t)\\ &= \sum_{i=1}^{2}\rho_i[(\Xi\bar{A}_i-L_{1i}\bar{C})e(t)+(\Xi\bar{B}_i-G_i)u(t)+\Xi\bar{D}\bar{d}(t)\\ &+\Xi\bar{g}(A_0\bar{x},t)-N_i\bar{g}(A_0\hat{\bar{x}},t)+(\Xi\bar{A}_i-L_{1i}\bar{C}-M_i)z(t)\\ &+((\Xi\bar{A}_i-L_{1i}\bar{C})H-L_{2i})y(t)-L_{1i}\omega(t)-H\dot{\omega}(t)]\end{aligned} \tag{14}$$

where $\Xi = I_6-H\bar{C}, L_i = L_{1i}+L_{2i}$.

If one can make the decoupling conditions hold at $\forall i=1,2$

$$\begin{aligned}M_i &= \Xi\bar{A}_i-L_{1i}\bar{C}\\ N_i &= \Xi\\ G_i &= \Xi\bar{B}_i\\ L_{2i} &= (\Xi\bar{A}_i-L_{1i}\bar{C})H\end{aligned} \tag{15}$$

Under these conditions, the state estimation error dynamics (14) is simplified as

$$\begin{aligned}\dot{e}(t) = \sum_{i=1}^{2}\rho_i[&(\Xi\bar{A}_i-L_{1i}\bar{C})\bar{e}(t)+\Xi\Delta\bar{g}+\Xi\bar{D}\bar{d}(t)\\ &-L_{1i}\omega(t)-H\dot{\omega}(t)]\end{aligned} \tag{16}$$

where $\Delta\bar{g} = \bar{g}(A_0\bar{x},t)-\bar{g}(A_0\hat{\bar{x}},t)$.

Proposition 1: For augmented system (11), there exists an LPV model based UIO in the form of (12) such that $\|e(t)\|_\infty \le \gamma\|\bar{d}_1\|_\infty$, if there exists the positive definite matrix P and matrices $Q_1, Q_{2i}, i=1,2,\cdots,r$, and scalar $\varepsilon>0$ such that

$$\begin{bmatrix}\Theta & P\bar{D}-Q_1\bar{C}\bar{D} & P-Q_1\bar{C} & -Q_{2i} & -Q_1\\ * & -\gamma^2 I & 0 & 0 & 0\\ * & * & -\varepsilon I & 0 & 0\\ * & * & * & -\gamma^2 I & 0\\ * & * & * & * & -\gamma^2 I\end{bmatrix} < 0 \tag{17}$$

where

$\Theta = (P\bar{A}_i-Q_1\bar{C}\bar{A}_i-Q_{2i}\bar{C})+(P\bar{A}_i-Q_1\bar{C}\bar{A}_i-Q_{2i}\bar{C})^T+(\varepsilon\theta^2+1)I$,

$Q_1 = PH, Q_{2i} = PL_{1i}$, $\bar{d}_1 = \begin{bmatrix}\bar{d}^T & \omega^T & \dot{\omega}^T\end{bmatrix}^T$, and γ is a performance index.

Proof: Select the following Lyapunov function for state estimation error dynamics (16)

$$V(t) = e^T Pe \tag{18}$$

Using (16) and (18), one has

$$\begin{aligned}\dot{V}(t) &= e^T P\dot{e}+\dot{e}^T Pe\\ &= \sum_{i=1}^{r}\rho_i\{e^T[P(\Xi\bar{A}_i-L_{1i}\bar{C})+(\Xi\bar{A}_i-L_{1i}\bar{C})^T P]e\\ &+2e^T P\Xi\bar{D}\bar{d}-2e^T PL_{1i}\omega-2e^T PH\dot{\omega}\\ &+e^T P\Xi\Delta\bar{g}+\Delta\bar{g}^T\Xi^T Pe\}\end{aligned} \tag{19}$$

For any matrices X, Y, and a positive scalar ε, following inequality holds[38]

$$X^TY+Y^TX \le \varepsilon X^TX+\varepsilon^{-1}Y^TY \tag{20}$$

Applying (20) to the last two terms in (19) and using Assumption 2, one has

$$e^T P\Xi\Delta\bar{g}+\Delta\bar{g}^T\Xi^T Pe \le \varepsilon\theta^2 e^T e+\varepsilon^{-1}e^T P\Xi\Xi^T Pe \tag{21}$$

Substituting (21) to (19), getting

$$\begin{aligned}\dot{V}(t) \le \sum_{i=1}^{r}\rho_i\{&e^T[P(\Xi\bar{A}_i-L_{1i}\bar{C})+(\Xi\bar{A}_i-L_{1i}\bar{C})^T P\\ &+\varepsilon\theta^2 I+\varepsilon^{-1}P\Xi\Xi^T P]e+2e^T P\Xi\bar{D}\bar{d}\\ &-2e^T PL_{1i}\omega-2e^T PH\dot{\omega}\}\end{aligned} \tag{22}$$

To guarantee the robustness of the designed LPV model based UIO against unknown external disturbance $\bar{d}_1(t)$, define the H_∞ performance index as

$$J = \int_0^\infty (e^T e-\gamma^2\bar{d}_1^T\bar{d}_1)dt \tag{23}$$

Using zero-initial condition (i.e. $V(0)=0, V(\infty)>0$), getting

$$\begin{aligned}J &= \int_0^\infty (e^T e-\gamma^2\bar{d}_1^T\bar{d}_1+\dot{V})dt+V(0)-V(\infty)\\ &\le \int_0^\infty (e^T e-\gamma^2\bar{d}_1^T\bar{d}_1+\dot{V})dt\\ &= \int_0^\infty\sum_{i=1}^{r}\rho_i[e^T(P(\Xi\bar{A}_i-L_{1i}\bar{C})+(\Xi\bar{A}_i-L_{1i}\bar{C})^T P\\ &+(\varepsilon\theta^2+1)I+\varepsilon^{-1}P\Xi\Xi^T P)e+2e^T P\Xi\bar{D}\bar{d}\\ &-2e^T PL_{1i}\omega-2e^T PH\dot{\omega}-\gamma^2\bar{d}_1^T\bar{d}_1]dt\\ &= \int_0^\infty\sum_{i=1}^{r}\rho_i\begin{bmatrix}e\\ \bar{d}\\ \omega\\ \dot{\omega}\end{bmatrix}^T\begin{bmatrix}\Omega & P\Xi\bar{D} & -PL_{1i} & -PH\\ * & -\gamma^2 I & 0 & 0\\ * & * & -\gamma^2 I & 0\\ * & * & * & -\gamma^2 I\end{bmatrix}\begin{bmatrix}e\\ \bar{d}\\ \omega\\ \dot{\omega}\end{bmatrix}dt\\ &= \sum_{i=0}^{r}\rho_i\int_0^\infty\begin{bmatrix}e\\ \bar{d}\\ \omega\\ \dot{\omega}\end{bmatrix}^T\begin{bmatrix}\Omega & P\Xi\bar{D} & -PL_{1i} & -PH\\ * & -\gamma^2 I & 0 & 0\\ * & * & -\gamma^2 I & 0\\ * & * & * & -\gamma^2 I\end{bmatrix}\begin{bmatrix}e\\ \bar{d}\\ \omega\\ \dot{\omega}\end{bmatrix}dt\end{aligned} \tag{24}$$

where

$$\begin{aligned}\Omega = &P(\Xi\bar{A}_i-L_{1i}\bar{C})+(\Xi\bar{A}_i-L_{1i}\bar{C})^T P\\ &+(\varepsilon\theta^2+1)I+\varepsilon^{-1}P\Xi\Xi^T P\end{aligned}$$

If the following inequality holds:

$$\begin{bmatrix}\Omega & P\Xi\bar{D} & -PL_{1i} & -PH\\ * & -\gamma^2 I & 0 & 0\\ * & * & -\gamma^2 I & 0\\ * & * & * & -\gamma^2 I\end{bmatrix} < 0 \tag{25}$$

1083-4435 (c) 2021 IEEE. Personal use is permitted, but republication/redistribution requires IEEE permission. See http://www.ieee.org/publications_standards/publications/rights/index.html for more information.

This article has been accepted for publication in a future issue of this journal, but has not been fully edited. Content may change prior to final publication. Citation information: DOI 10.1109/TMECH.2021.3087193, IEEE/ASME Transactions on Mechatronics

then one has $\|e(t)\|_\infty \le \gamma \|\bar{d}_1\|_\infty$.

Applying the Schur complement lemma, inequality (25) is described as

$$\begin{bmatrix} \Theta & P\Xi D & P\Xi & -PL_{1i} & -PH \\ * & -\gamma^2 I & 0 & 0 & 0 \\ * & * & -\varepsilon I & 0 & 0 \\ * & * & * & -\gamma^2 I & 0 \\ * & * & * & * & -\gamma^2 I \end{bmatrix} < 0 \quad (26)$$

where $\Theta = P(\Xi\bar{A}_i - L_{1i}\bar{C}) + (\Xi\bar{A}_i - L_{1i}\bar{C})^T P + (\varepsilon\theta^2 + 1)I$.

If let $Q_1 = PH, Q_{2i} = PL_{1i}$, it follows that (26) is equivalent to (17), thus completing the proof.

For the purpose of ensuring the convergence rate of the proposed robust LPV model based UIO, pole placement technique is futher introduced to configure all the eigenvalues of matrix $(\Xi\bar{A}_i - L_{1i}\bar{C})$ into a stable circular area, $D(\sigma,\tau)$. Thus, the following inequality is added as an additional condition along with inequality (17).

$$\begin{bmatrix} -P & P\bar{A}_i - Q_1\bar{C}\bar{A}_i - Q_{2i}\bar{C} - \sigma P \\ * & -\tau^2 P \end{bmatrix} < 0 \quad (27)$$
$$i = 1, \cdots, r.$$

where σ is the centre of the circle to be designed, and τ is the radius.

Based on Proposition 1 and condition (27), a robust LPV model based UIO (12) is implemented and the augmented estimate $\hat{\bar{x}}$ is obtained, leading to the fault estimate as follows:

$$\hat{f}_a = \begin{bmatrix} 0_{2\times 4} & I_2 \end{bmatrix} \hat{\bar{x}} \quad (28)$$

IV. SIMULATION AND EXPERIMENTAL RESULTS

Simulation and experimental tests are all conducted to show the effectiveness and performance of the proposed fault estimation design. High-gain observer (HGO)[31] and modified PID observer (MPIDO)[30] are selected for comparative analysis. The experimental platform is shown in Fig. 2. A data acquisition board Q8-USB is adopted to collect analog signals from the helicopter and convert them to digital signals, and a power amplifier VoltPAQ-X2 is adopted for the power output. Two encoders with high resolution are used to measure the elevation and pitch angles[39]. The controller and proposed fault observer are implemented via Matlab 2017a with Quarc 2.7, which are taken as Simulink programming environment. The simulation and experiment adopt a fixed step size, and the sampling time was set at 0.001s. The system parameter of the 3-DOF helicopter is not presented here, which can be found in Quanser's 3-DOF helicopter user manual or some existing papers[39][40].

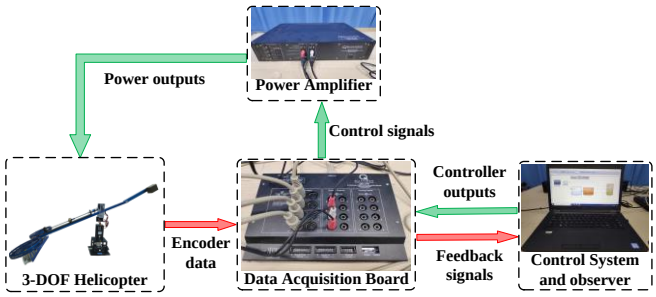

Fig 2. 3-DOF helicopter experimental system

In the 3-DOF helicopter prototype, initial value of elevation and pitch angles are -27.5 ° and 0 ° respectively. Assume that both the front and rear actuators of the helicopter have additive faults in the following form

$$f_{a1} = \begin{cases} 0, & 0 < t < 20 \\ 0.4(\text{t-20}), & 20 \le t < 30 \\ -0.4(t-40), & 30 \le t < 40 \\ 0, & 40 \le t < 80 \end{cases} \quad (29)$$

$$f_{a2} = \begin{cases} 0, & 0 < t < 50 \\ \text{-0.4(t-50)}, & 50 \le t < 60 \\ 0.4(t-70), & 60 \le t < 70 \\ 0, & 70 \le t < 80 \end{cases} \quad (30)$$

Remark 4: The fault signals considered here are continuous, but not differentiable at the mutation point, which is inconsistent with Assumption 1. Assumption 1 is strict because there is no known prior knowledge of the fault signal bound in practice. However, we can determine that there is an upper bound on the fault signal.

(1) LPV model based unknown input observer design

Choosing $\gamma = 0.1$, ε=0.001, $\sigma = -10$, and $\tau = 5$, the observer gain matrices are calculated as follows

$$M_1 = \begin{bmatrix} -7.93 & 0 & 0 & 0 & 0 & 0 \\ 0 & -7.93 & 0 & 0 & 0 & 0 \\ 0 & 0 & -7.93 & 0 & 0 & 0 \\ 0 & 0 & 0 & -7.93 & 0 & 0 \\ 0 & 0 & -1.50 & -0.18 & -2.32 & 0.60 \\ 0 & 0 & -1.50 & 0.18 & 0.60 & -2.32 \end{bmatrix}, G_1 = \begin{bmatrix} 0 & 0 \\ 0 & 0 \\ 0 & 0 \\ 0 & 0 \\ -2.32 & 0.60 \\ 0.60 & -2.32 \end{bmatrix}$$

$$M_2 = \begin{bmatrix} -7.93 & 0 & 0 & 0 & 0 & 0 \\ 0 & -7.93 & 0 & 0 & 0 & 0 \\ 0 & 0 & -7.93 & 0 & 0 & 0 \\ 0 & 0 & 0 & -7.93 & 0 & 0 \\ 0 & 0 & -1.12 & -0.18 & -1.90 & 1.02 \\ 0 & 0 & -1.12 & 0.18 & 1.02 & -1.90 \end{bmatrix}, G_2 = \begin{bmatrix} 0 & 0 \\ 0 & 0 \\ 0 & 0 \\ 0 & 0 \\ -1.90 & 1.02 \\ 1.02 & -1.90 \end{bmatrix}$$

$$N_1 = \begin{bmatrix} 0 & 0 & 0 & 0 & 0 & 0 \\ 0 & 0 & 0 & 0 & 0 & 0 \\ 0 & 0 & 0 & 0 & 0 & 0 \\ 0 & 0 & 0 & 0 & 0 & 0 \\ 0 & 0 & -10.05 & -2.51 & 1 & 0 \\ 0 & 0 & -10.05 & 2.51 & 0 & 1 \end{bmatrix}, N_2 = \begin{bmatrix} 0 & 0 & 0 & 0 & 0 & 0 \\ 0 & 0 & 0 & 0 & 0 & 0 \\ 0 & 0 & 0 & 0 & 0 & 0 \\ 0 & 0 & 0 & 0 & 0 & 0 \\ 0 & 0 & -7.30 & -2.51 & 1 & 0 \\ 0 & 0 & -7.30 & 2.51 & 0 & 1 \end{bmatrix}$$

1083-4435 (c) 2021 IEEE. Personal use is permitted, but republication/redistribution requires IEEE permission. See http://www.ieee.org/publications_standards/publications/rights/index.html for more information.

This article has been accepted for publication in a future issue of this journal, but has not been fully edited. Content may change prior to final publication. Citation information: DOI 10.1109/TMECH.2021.3087193, IEEE/ASME Transactions on Mechatronics

$$L_1=\begin{bmatrix}0&0&0&0&0&0\\0&0&0&0&0&0\\0&0&0&0&0&0\\0&0&0&0&0&0\\0&0&0&0&-17.33&-7.34\\0&0&0&0&-17.33&7.34\end{bmatrix}\quad L_2=\begin{bmatrix}0&0&0&0&0&0\\0&0&0&0&0&0\\0&0&0&0&0&0\\0&0&0&0&0&0\\0&0&0&0&-6.46&-7.34\\0&0&0&0&-6.46&7.34\end{bmatrix}$$

$$H=\begin{bmatrix}1&0&0&0\\0&1&0&0\\0&0&1&0\\0&0&0&1\\0&0&7.30&2.51\\0&0&7.30&-2.51\end{bmatrix}$$

(2) High gain observer design

Define an augmented system state as

$$\bar{x}=\begin{bmatrix}x^T & f_a{}^T & \omega^T\end{bmatrix}^T \tag{31}$$

The equivalent system established by (3) and (31) is as follows

$$\begin{aligned}&\bar{E}\dot{\bar{x}}=\bar{A}\bar{x}+\bar{B}u+\bar{D}d+\bar{M}(\alpha f_a+\dot{f}_a)+\bar{N}\omega+\bar{g}(A_1\bar{x})\\&y=\bar{C}\bar{x}\end{aligned} \tag{32}$$

where α is a scalar and

$$\bar{E}=\begin{bmatrix}I_4&0&0\\0&I_2&0\\0&0&0\end{bmatrix},\bar{A}=\begin{bmatrix}A&B&0\\0&-\alpha I_2&0\\0&0&-I_4\end{bmatrix},\bar{B}=\begin{bmatrix}B\\0\\0\end{bmatrix},\bar{D}=\begin{bmatrix}D\\0\\0\end{bmatrix},$$

$$\bar{M}=\begin{bmatrix}0\\I_2\\0\end{bmatrix},\bar{N}=\begin{bmatrix}0\\0\\I_4\end{bmatrix},\bar{C}=\begin{bmatrix}C&0&I_4\end{bmatrix},A_1=\begin{bmatrix}I_4&0&0\end{bmatrix}.$$

Consider the following high gain observer:

$$\begin{aligned}&\bar{S}\dot{\xi}=(\bar{A}-\bar{K}\bar{C})\xi+\bar{B}u-\bar{N}y+\bar{g}(A_1\hat{\bar{x}})\\&\hat{\bar{x}}=\xi+\bar{S}^{-1}\bar{L}y\end{aligned} \tag{33}$$

where ξ is the system state of the observer (33), $\hat{\bar{x}}$ is the estimation of $\bar{x}$, and the gain matrices $\bar{S}=\bar{E}+\bar{L}\bar{C}$, $\bar{K},\bar{L}$ are to be designed.

In this paper, choosing $\alpha=0.01$, the gain matrices are calculated as follows:

$$\bar{L}=\begin{bmatrix}0&0&0&0\\0&0&0&0\\0&0&0&0\\0&0&0&0\\0&0&0&0\\0&0&0&0\\100&0&0&0\\0&100&0&0\\0&0&100&0\\0&0&0&100\end{bmatrix},\ \bar{K}=10^8\times\begin{bmatrix}0.01&0&0.0003&0\\0&0.01&0&0.0003\\0.0001&0&0.03&0\\0&0.0001&0&0.03\\0&0&5.8303&0.8598\\0&0&5.8203&-0.8605\\0.0002&0&0&0\\0&0.0002&0&0\\0&0&0.0003&0\\0&0&0&0.0003\end{bmatrix}$$

$$\bar{S}=\begin{bmatrix}1&0&0&0&0&0&0&0&0&0\\0&1&0&0&0&0&0&0&0&0\\0&0&1&0&0&0&0&0&0&0\\0&0&0&1&0&0&0&0&0&0\\0&0&0&0&1&0&0&0&0&0\\0&0&0&0&0&1&0&0&0&0\\100&0&0&0&0&0&100&0&0&0\\0&100&0&0&0&0&0&100&0&0\\0&0&100&0&0&0&0&0&100&0\\0&0&0&100&0&0&0&0&0&100\end{bmatrix}$$

(3) Modified PID observer design

The augmented system state can be defined as

$$\bar{x}=\begin{bmatrix}x^T & \omega^T\end{bmatrix}^T \tag{34}$$

A augmented system can be obtained from (3) and (34)

$$\begin{aligned}&\bar{E}\dot{\bar{x}}=\bar{A}\bar{x}+\bar{B}u+\bar{N}\omega+\bar{B}f_a+\bar{D}d+\bar{g}(A_2\bar{x})\\&y=\bar{C}\bar{x}\end{aligned} \tag{35}$$

where

$$\bar{E}=\begin{bmatrix}I_4&0\\0&0\end{bmatrix},\bar{A}=\begin{bmatrix}A&0\\0&-I_4\end{bmatrix},\bar{B}=\begin{bmatrix}B\\0\end{bmatrix},\bar{D}=\begin{bmatrix}D\\0\end{bmatrix},\bar{N}=\begin{bmatrix}0\\I_4\end{bmatrix},$$

$$\bar{C}=\begin{bmatrix}C&I_4\end{bmatrix},A_2=\begin{bmatrix}I_4&0\end{bmatrix}.$$

Consider the following modified proportional integral derivative observer:

$$\begin{aligned}&(\bar{E}+\bar{L}\bar{C})\dot{\xi}=(\bar{A}-\bar{K}\bar{C})\xi+\bar{B}u+\bar{A}(\bar{E}+\bar{L}\bar{C})^{-1}\bar{L}y+\bar{B}\hat{f}_a+\bar{g}(A_1\hat{\bar{x}})\\&\dot{\hat{f}}_a(t)=-K_I C\xi\\&\hat{\bar{x}}(t)=\xi+(\bar{E}+\bar{L}\bar{C})^{-1}\bar{L}y\end{aligned} \tag{36}$$

where ξ is the system state of the observer (36), $\hat{\bar{x}}$ is the estimation of $\bar{x}$, $\hat{f}_a$ is the estimation of f_a, and $\bar{L}=\begin{bmatrix}L_1^T & L_2^T\end{bmatrix}^T$, the gain matrices $L_1,L_2,\bar{K},K_I$ are to be designed.

In this paper, choose

$$\bar{L}=\begin{bmatrix}L_1\\L_2\end{bmatrix}=\begin{bmatrix}0&0&0&0\\0&0&0&0\\0&0&0&0\\0&0&0&0\\10000&0&0&0\\0&10000&0&0\\0&0&10000&0\\0&0&0&10000\end{bmatrix}$$

such that $(\bar{E}+\bar{L}\bar{C})$ is nonsingular. Then, the design matrices are obtained as follows:

$$\bar{K}=10^7\times\begin{bmatrix}0.4499&0.0400&0.0542&-0.0539\\0.0129&0.4464&0.0091&-0.0196\\-0.4210&-0.0794&0.8707&-0.0739\\0.0982&-0.5051&0.0573&1.0856\\0.0442&0.0017&0.0014&-0.0018\\0.0005&0.0433&0.0003&-0.0028\\-0.0109&-0.0014&0.0533&-0.0014\\0.0042&-0.0133&0.0019&0.0592\end{bmatrix},$$

$$K_I=10^8\times\begin{bmatrix}-2.0261&-0.5634&2.6330&-0.0404\\-2.0733&0.1738&2.5563&-1.0767\end{bmatrix}.$$

1083-4435 (c) 2021 IEEE. Personal use is permitted, but republication/redistribution requires IEEE permission. See http://www.ieee.org/publications_standards/publications/rights/index.html for more information.

This article has been accepted for publication in a future issue of this journal, but has not been fully edited. Content may change prior to final publication. Citation information: DOI 10.1109/TMECH.2021.3087193, IEEE/ASME Transactions on Mechatronics

To verify the fault estimation performance of proposed method, two simulation cases and two experiment cases are conducted.

Remark 5: In 3-DOF helicopter platform, when the pitch angle is greater than $15°$, actuator saturation will occur in the system, which will seriously influence the performance of the fault observer. Furthermore, when the pitch angle is set too large, the helicopter rotates too fast in the experiment, which is dangerous to some extent. Therefore, the pitch angle is constrained within $[0°,15°]$.

A. *Simulation test under mild maneuvers*

To verify the performance of the designed observer in eliminating measurement noises, a comparative simulation test is carried out when the pitch angle is $0°$. In this simulation, a Gaussian noise with form $N(0,0.001^2)$ is added to the helicopter output.

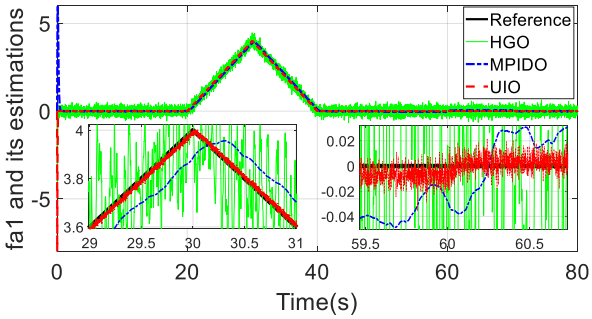

Fig 3. Estimation results of f_{a1} (p=0° , simulation results)

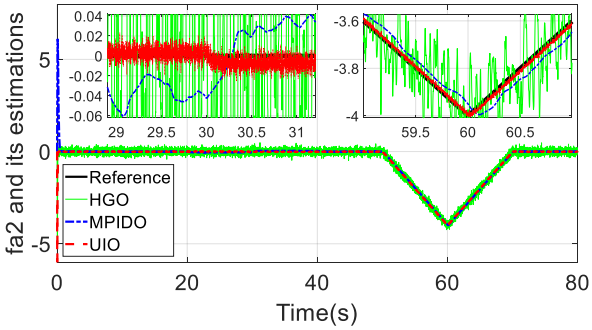

Fig 4. Estimation results of f_{a2} (p=0° , simulation results)

From Figs. 3 and 4, the fault estimation results of the high gain observer are seriously affected by measurement noises and contain many high frequency components. The modified PID observer and UIO can handle the negative effects of measurement noises and result good fault estimation results. However, obvious estimation errors of actuator fault in both front and back motor can be found during 20s-40s by using modified PID observer. From 50s-70s, it can be seen that the performance of modified PID observer is also very poor. And it can be concluded that actuator faults in front and back motor are interacted with each other. Comparatively, the LPV model based UIO is only slightly affected by the measurement noises, which results best fault estimation performance in the three fault estimation approaches.

B. *Experimental test under mild maneuver*

To further verify and compare the performance of three observers in eliminating measurement noises, experimental tests are conducted under mild maneuver, in which the pitch angle of the 3-DOF helicopter is very small.

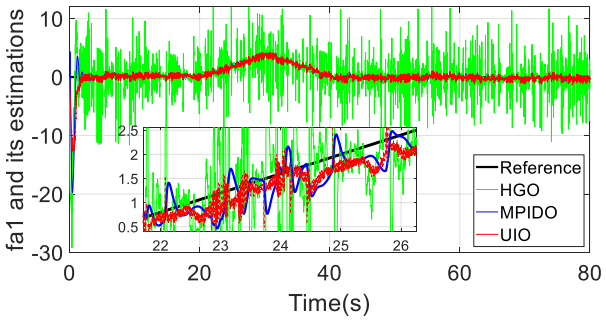

Fig 5. Estimation results of f_{a1} (p=0° , experimental results)

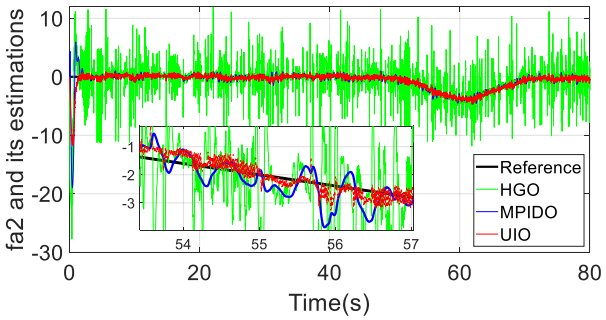

Fig 6. Estimation results of f_{a2} (p=0° ,experimental results)

The experimental results of three fault estimation approaches are shown in Figs. 5 and 6. The experiment results of the high gain observer are consistent with the simulation results, which are seriously affected by measurement noises. The modified PID observer can well eliminate the influence of measurement noise. However, it has a large fault estimation error. Consistent with the simulation results, the LPV model based UIO can effectively suppress the influence of measurement noises, and the fault estimation error is also minimal. Thus, the effectiveness of the LPV model based UIO in actuator faults estimation under measurement noises is well verified.

C. *Simulation test under aggressive maneuvers*

To further validate the effectiveness of the proposed robust fault observer under aggressive maneuvers, comparative simulations are conducted. The performance of the proposed approach is demonstrated when pitch angle is $0°$, $10°$ and $15°$ respectively. Furthermore, a comparative study is performed with a UIO adopted in [24] to highlight the advantages of the proposed observer.

1083-4435 (c) 2021 IEEE. Personal use is permitted, but republication/redistribution requires IEEE permission. See http://www.ieee.org/publications_standards/publications/rights/index.html for more information.

This article has been accepted for publication in a future issue of this journal, but has not been fully edited. Content may change prior to final publication. Citation information: DOI 10.1109/TMECH.2021.3087193, IEEE/ASME Transactions on Mechatronics

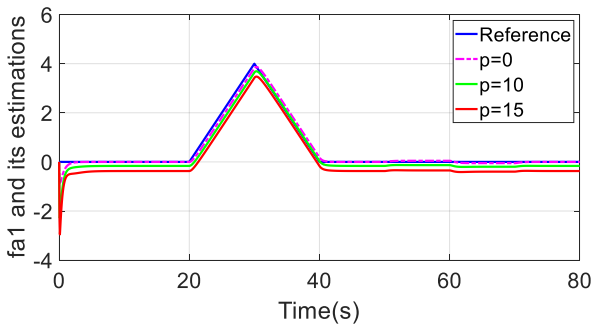

Fig 7. Estimation results of f_{a1} with UIO[24] (simulation results)

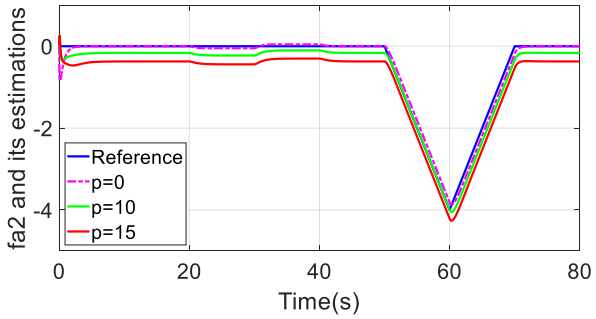

Fig 8. Estimation results of f_{a2} with UIO[24] (simulation results)

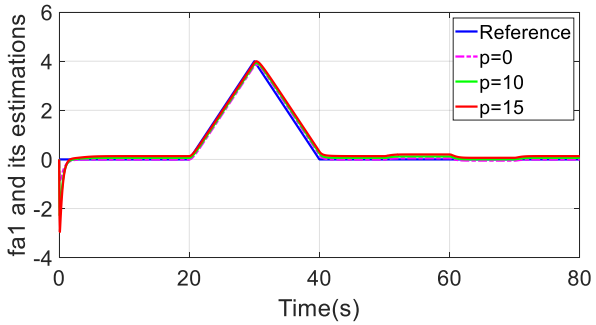

Fig 9. Estimation results of f_{a1} with LPV model based UIO (simulation results)

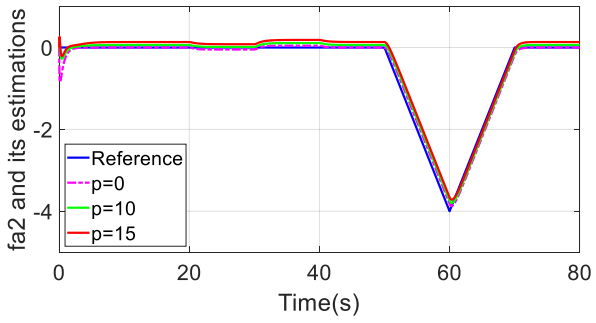

Fig 10. Estimation results of f_{a2} with LPV model based UIO (simulation results)

From Figs. 7 and 8, it can be seen that actuator faults in both front and back motor can be well estimated when the pitch angle is $0°$. When the pitch angle increases, obvious steady state error can be found in the fault estimation results, and these error increases as the pitch angle increases. This is mainly because the interaxis nonlinear coupling effect is not considered in the conventional UIO design[24], which can deteriorate the fault estimation performance. However, as it is shown in Figs. 9 and 10, LPV model based UIO is capable of addressing the interaxis nonlinear coupling. Small estimation error can be still restrained in spite of pitch angle change.

D. Experimental test under aggressive maneuvers

Experimental tests are carried out on the 3-DOF helicopter system. From Figs. 11 and 12, it can be seen that the UIO adopt in [24] can estimate two faults well when the pitch angle is $0°$. However, because the interaxis nonlinear coupling is not considered in [24], there is obvious steady state error when the pitch angle is large, and the error will increases as the pitch angle is becoming larger. Figs. 13 and 14 demonstrate that LPV model based UIO can accurately estimate two faults, even at large pitch angles. Therefore, LPV model based UIO can obtain good fault estimation performances when the helicopter system operates in aggressive maneuvers.

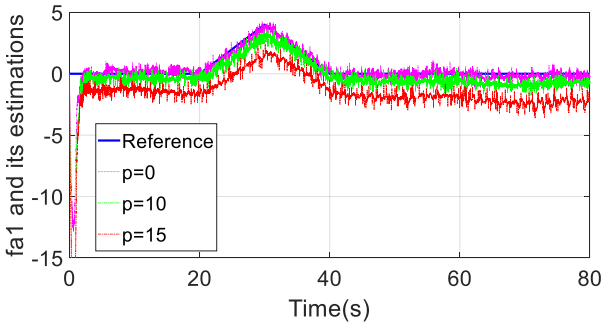

Fig 11. Estimation results of f_{a1} with UIO[24] (experimental results)

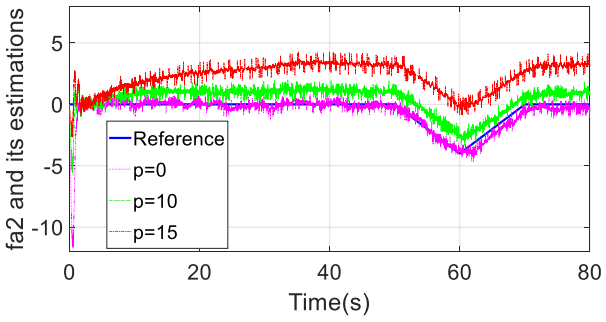

Fig 12. Estimation results of f_{a2} with UIO[24] (experimental results)

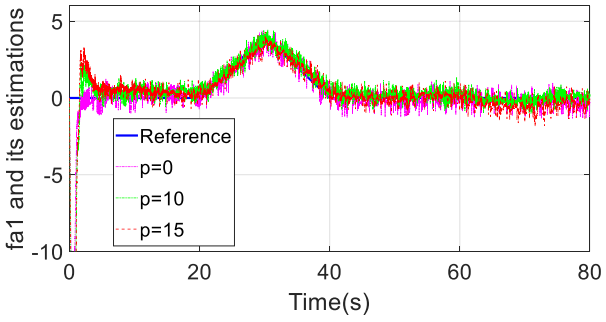

Fig 13. Estimation results of f_{a1} with LPV model based UIO (experimental results)

1083-4435 (c) 2021 IEEE. Personal use is permitted, but republication/redistribution requires IEEE permission. See http://www.ieee.org/publications_standards/publications/rights/index.html for more information.

This article has been accepted for publication in a future issue of this journal, but has not been fully edited. Content may change prior to final publication. Citation information: DOI 10.1109/TMECH.2021.3087193, IEEE/ASME Transactions on Mechatronics

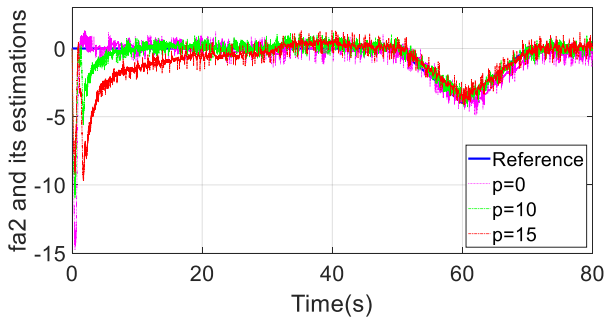

Fig 14. Estimation results of f_{a2} with LPV model based UIO (experimental results)

V. CONCLUSIONS

This paper proposes a robust actuator fault estimation approach for the 3-DOF helicopter system considering measurement noises under aggressive maneuvers. Measurement noises are considered in fault estimation of a 3-DOF helicopter prototype. And a modified polytopic LPV model is developed for 3-DOF helicopter system to cope with the interaxis nonlinear coupling under aggressive maneuvers. Based on the modified polytopic LPV model, a robust LPV model based UIO is designed to estimate actuator fault. Energy-to-energy strategy is adopted to restrain the negative effects of measurement noises on the robust performance of proposed fault observer. Based on a 3-DOF helicopter prototype, both simulations and experiments are carried out. And the advantage of the proposed method is sufficiently validated by using comparative analysis. It demonstrates that the designed observer is robust to measurement noises and can achieve higher estimation accuracy and smaller estimation error under aggressive maneuvers. The focus of future work is to reduce the convergence time and overshoot of the proposed fault estimation approach.

REFERENCES

[1] Santoso F, Garratt M. A, Anavatti S. G, et al. Entropy Fuzzy System Identification for the Heave Flight Dynamics of a Model-Scale Helicopter[J]. IEEE/ASME Transactions on Mechatronics, 2019, 25(5): 2330-2341.

[2] O. Kose, T. Oktay. Simultaneous quadrotor autopilot system and collective morphing system design[J]. Aircraft Engineering and Aerospace Technology, 2020, 92(7): 1093–1100.

[3] O. Kose, T. Oktay. Lateral Control with Differential and Collective Morphing in Quadrotors[J]. Journal of Aviation, 2020, 4(2): 48–54.

[4] Yang H, Jiang B, Liu H. H. T., et al. Attitude Synchronization For Multiple 3-DOF Helicopters With Actuator Faults[J]. IEEE/ASME Transactions on Mechatronics, 2019, 24(2): 597-608.

[5] Chung W and Son H. Fault-Tolerant Control of Multirotor UAVs by Control Variable Elimination[J]. IEEE/ASME Transactions on Mechatronics, 2020, 25(5): 2513-2522.

[6] Ma H J, Liu Y, Li T, et al. Nonlinear high-gain observer-based diagnosis and compensation for actuator and sensor faults in a quadrotor unmanned aerial vehicle[J]. IEEE Transactions on Industrial Informatics, 2018, 15(1): 550-562.

[7] Freeman P, Pandita R, Srivastava N, et al. Model-based and data-driven fault detection performance for a small UAV[J]. IEEE/ASME Transactions on mechatronics, 2013, 18(4): 1300-1309.

[8] Avram R C, Zhang X, Muse J. Quadrotor actuator fault diagnosis and accommodation using nonlinear adaptive estimators[J]. IEEE Transactions on Control Systems Technology, 2017, 25(6): 2219-2226.

[9] Yao Y X, Radun A V. Proportional integral observer design for linear systems with time delay[J]. IET Control Theory & Applications, 2007, 1(4): 887-892.

[10] Fu S, Qiu J, Chen L, et al. Adaptive fuzzy observer design for a class of switched nonlinear systems with actuator and sensor faults[J]. IEEE Transactions on Fuzzy Systems, 2018, 26(6): 3730-3742.

[11] Nahian S A , Dinh T Q , Dao H V , et al. An Unknown Input Observer-EFIR Combined Estimator for Electro-Hydraulic Actuator in Sensor Fault Tolerant Control Application[J]. IEEE/ASME Transactions on Mechatronics, 2020, 25(2):2208-2219.

[12] Gao Z, Liu X, Chen M Z Q. Unknown input observer-based robust fault estimation for systems corrupted by partially decoupled disturbances[J]. IEEE Transactions on Industrial Electronics, 2015, 63(4): 2537-2547.

[13] Jia Q, Chen W, Zhang Y, et al. Robust fault reconstruction via learning observers in linear parameter-varying systems subject to loss of actuator effectiveness[J]. IET Control Theory & Applications, 2014, 8(1): 42-50.

[14] Yang H, Yin S. Reduced-Order Sliding-Mode-Observer-Based Fault Estimation for Markov Jump Systems[J]. IEEE Transactions on Automatic Control, 2019, 64(11): 4733-4740.

[15] Pourbabaee B, Meskin N, Khorasani K. Sensor fault detection, isolation, and identification using multiple-model-based hybrid Kalman filter for gas turbine engines[J]. IEEE Transactions on Control Systems Technology, 2015, 24(4): 1184-1200.

[16] Chen F, Jiang R, Zhang K, et al. Robust backstepping sliding-mode control and observer-based fault estimation for a quadrotor UAV[J]. IEEE Transactions on Industrial Electronics, 2016, 63(8): 5044-5056.

[17] Zhong Y, Zhang Y, Zhang W, et al. Actuator and Sensor Fault Detection and Diagnosis for Unmanned Quadrotor Helicopters[J]. IFAC-Papers OnLine, 2018, 51(24): 998-1003.

[18] Abbaspour A, Aboutalebi P, Yen K K, et al. Neural adaptive observer-based sensor and actuator fault detection in nonlinear systems: Application in UAV[J]. ISA transactions, 2017, 67: 317-329.

[19] Nian X, Chen W, Chu X, et al. Robust adaptive fault estimation and fault tolerant control for quadrotor attitude systems[J]. International Journal of Control, 2020, 93(3): 725-737.

[20] Chen F, Zhang K, Jiang B, et al. Adaptive sliding mode observer-based robust fault reconstruction for a helicopter with actuator fault[J]. Asian Journal of Control, 2016, 18(4): 1558-1565.

[21] Chen M, Shi P, Lim C C. Adaptive neural fault-tolerant control of a 3-DOF model helicopter system[J]. IEEE Transactions on Systems, Man, and Cybernetics: Systems, 2015, 46(2): 260-270.

[22] De Loza A F, Cieslak J, Henry D, et al. Output tracking of systems subjected to perturbations and a class of actuator faults based on HOSM observation and identification[J]. Automatica, 2015, 59: 200-205.

[23] Zeghlache S, Benslimane T, Bouguerra A. Active fault tolerant control based on interval type-2 fuzzy sliding mode controller and non linear adaptive observer for 3-DOF laboratory helicopter[J]. ISA transactions, 2017, 71: 280-303.

[24] Lan J, Patton R J, Zhu X. Integrated fault-tolerant control for a 3-DOF helicopter with actuator faults and saturation[J]. IET Control Theory & Applications, 2017, 11(14): 2232-2241.

[25] Cai G, Chen B M, Dong X, et al. Design and implementation of a robust and nonlinear flight control system for an unmanned helicopter[J]. Mechatronics, 2011, 21(5): 803-820.

[26] Ferruz J, Vega V M, Ollero A, et al. Reconfigurable control architecture for distributed systems in the HERO autonomous helicopter[J]. IEEE Transactions on Industrial Electronics, 2010, 58(12): 5311-5318.

[27] Lu M , Zhu X , Wang T . Comparative study of fault estimation for 3-DOF helicopter[C]. in Proc. of 39th Chinese Control Conference, IEEE, 2020, pp. 4060–4065.

[28] Zheng B, Zhong Y. Robust attitude regulation of a 3-DOF helicopter benchmark: theory and experiments[J]. IEEE transactions on industrial electronics, 2010, 58(2): 660-670.

[29] Zhu X, Li D. Robust attitude control of a 3-DOF helicopter considering actuator saturation[J]. Mechanical Systems and Signal Processing, 2021, 149: 107209.

[30] Gao Z, Wang H. Descriptor observer approaches for multivariable systems with measurement noises and application in fault detection and diagnosis[J]. Systems & Control Letters, 2006, 55(4): 304-313.

[31] Gao Z, Breikin T, Wang H. High-gain estimator and fault-tolerant design with application to a gas turbine dynamic system[J]. IEEE Transactions on Control Systems Technology, 2007, 15(4): 740-753.

1083-4435 (c) 2021 IEEE. Personal use is permitted, but republication/redistribution requires IEEE permission. See http://www.ieee.org/publications_standards/publications/rights/index.html for more information.

This article has been accepted for publication in a future issue of this journal, but has not been fully edited. Content may change prior to final publication. Citation information: DOI 10.1109/TMECH.2021.3087193, IEEE/ASME Transactions on Mechatronics

[32] Ma T, Cao C. Estimation using L1 adaptive descriptor observer for multivariable systems with nonlinear uncertainties and measurement noises[J]. European Journal of Control, 2020, 52: 11-18.
[33] Liu H, Lu G, Zhong Y. Robust LQR attitude control of a 3-DOF laboratory helicopter for aggressive maneuvers[J]. IEEE Transactions on Industrial Electronics, 2013, 60(10): 4627-4636.
[34] Liu H, Tian Y, Lewis F, et al. Robust formation tracking control for multiple quadrotors under aggressive maneuvers[J]. Automatica, 2019, 105: 179-185.
[35] Zhu X, Li D. Robust fault estimation for a 3-DOF helicopter considering actuator saturation[J]. Mechanical Systems and Signal Processing, 2021, 155: 107624.
[36] Zhang H, Zhang G, Wang J. Hꝏ Observer Design for LPV Systems With Uncertain Measurements on Scheduling Variables: Application to an Electric Ground Vehicle[J]. IEEE/ASME Transactions on Mechatronics, 2016, 21(3): 1659-1670.
[37] Zhang H, Wang J. Active steering actuator fault detection for an automatically-steered electric ground vehicle[J]. IEEE Transactions on Vehicular Technology, 2016, 66(5): 3685-3702.
[38] Zhu X, Li W. Takagi–Sugeno fuzzy model based shaft torque estimation for integrated motor–transmission system[J]. ISA transactions, 2019, 93: 14-22.
[39] Quanser Inc. 3-DOF Helicopter User Manual, 2011.
[40] Yang X, Zheng X. Adaptive NN Backstepping Control Design for a 3-DOF Helicopter: Theory and Experiments[J]. IEEE Transactions on Industrial Electronics, 2020, 67(5): 3967-3979.

1083-4435 (c) 2021 IEEE. Personal use is permitted, but republication/redistribution requires IEEE permission. See http://www.ieee.org/publications_standards/publications/rights/index.html for more information.